

The G \bar{o} Model Revisited: Native Structure and the Geometric Coupling between Local and Long-Range Contacts

Patrícia F. N. Faisca,* Margarida M. Telo da Gama, and Ana Nunes

Centro de Física Teórica e Computacional da Universidade de Lisboa, Lisboa Codex, Portugal

ABSTRACT Monte Carlo simulations show that long-range interactions play a major role in determining the folding rates of 48-mer three-dimensional lattice polymers modeled by the G \bar{o} potential. For three target structures with different native geometries we found a sharp increase in the folding time when the relative contribution of the long-range interactions to the native state's energy is decreased from ~50% towards zero. However, the dispersion of the simulated folding times is strongly dependent on native geometry and G \bar{o} polymers folding to one of the target structures exhibits folding times spanning three orders of magnitude. We have also found that, depending on the target geometry, a strong geometric coupling may exist between local and long-range contacts, which means that, when this coupling exists, the formation of long-range contacts is forced by the previous formation of local contacts. The absence of a strong geometric coupling results in a kinetics that is more sensitive to the interaction energy parameters; in this case, the formation of local contacts is not capable of promoting the establishment of long-range ones when the latter are strongly penalized energetically and this results in longer folding times. *Proteins* 2005;60:712–722. © 2005 Wiley-Liss, Inc.

Key words: lattice models; Monte Carlo simulation; native geometry; folding kinetics

INTRODUCTION

In the last few years the idea that the native geometry governs the overall folding kinetics of small (typically with less than 100 amino acids), single domain, two-state proteins has attracted considerable attention and prompted several new lines of research.^{1–9} A particularly important observation by Plaxco et al.^{1,10} revealed the existence of a strong correlation ($r = 0.92$) between the experimental folding rates of 24 two-state folders and the so-called contact order parameter, CO, measuring the average sequence separation of contacting residue pairs in the native structure relative to the protein chain length. The connection between the CO (and in more general terms, the native geometry) and the average range of amino acid interactions in the native fold has set a new ground for discussing an old-debated issue in the protein folding literature, namely, that of understanding the roles of local (i.e., close in space and in sequence) and long-range (i.e.,

close in space but distant along the sequence) interresidue interactions in the folding dynamics. Results obtained within the scope of this debate agree on the idea that long-range (LR) interactions play an important role in stabilizing the native fold^{11–14} but there is no definite consensus on what is their role in the folding kinetics. For example, very early results obtained by G \bar{o} and Taketomi¹¹ for a 49-residue chain in a two-dimensional square lattice suggest that local interactions accelerate both the folding and unfolding transitions. In ref. 15, Unger and Moulton have studied optimized heteropolymer sequences with chain length $N = 27$ in a three-dimensional cubic lattice and concluded that increasing the strength of local interactions increases the ability of sequences to fold. In a different study,¹³ Doyle and coworkers have found that, in the context of the Zwanzig model, the rate of folding increases as the contribution of the local interactions to the native state's energy increases. By contrast, results obtained by Abkevich et al.¹² for the Miyazawa-Jernigan lattice-polymer model provided evidence that, under conditions where the native state is stable, a 36-residue sequence on a three-dimensional cubic lattice folds to a native structure with mostly LR contacts two orders of magnitude faster than a sequence folding to a native structure with predominantly local contacts. In ref.16, Govindarajan and Goldstein have used a lattice model in conjunction with techniques drawn from spin glasses theory and found that optimal conditions for folding are achieved when local interactions contribute little to the native state's energy. More recently, Gromiha and Selvaraj¹⁷ have analyzed the “global” contribution of LR interactions to the folding kinetics by introducing a new geometrical parameter named long-range order (LRO). The LRO, which measures the total number of LR contacts in the native structure relative to the protein chain length, was found to correlate as well as the CO with the folding rates of 23 (out of the 24) two-state folders previously studied by Plaxco et al.¹⁰ This observation emphasizes the

Grant sponsor: Fundação para a Ciência e a Tecnologia; Grant number: BPD10083/2002 (to P.F.N.F.)

*Correspondence to: Patrícia Faisca, Centro de Física Teórica e Computacional da Universidade de Lisboa, Av. Prof. Gama Pinto 2, 1649-003 Lisboa Codex, Portugal. E-mail: patnev@alf1.cii.fc.ul.pt

Received 26 November 2004; Revised 25 January 2005; Accepted 18 February 2005

Published online 14 July 2005 in Wiley InterScience (www.interscience.wiley.com). DOI: 10.1002/prot.20521

relative importance of LR interactions in protein folding kinetics.

In addition, it has been shown recently that the free energy landscapes of single domain, two-state folders are considerably smooth.^{22,23} This finding led to a renewed interest^{8,27,28} in the G \bar{o} model and other modified G \bar{o} -type interaction schemes because, as for simple proteins, their energy landscapes are relatively smooth.²⁸ Indeed, these models do not take into account the sequence's chemical composition and account only for attractive interactions between native contacts thereby eliminating possible energetic traps. As a consequence, only geometric traps, resulting from the chain connectivity and the geometry of the native fold, will contribute to the landscape's ruggedness and thus G \bar{o} -type models are said to be frustrated in a "topological" sense. These models are therefore particularly suited to investigate the role of the native state's geometry in the folding kinetics of simple proteins.

Motivated by these recent results, we revisit the G \bar{o} model to study the dependence of the folding kinetics on LR (and local) interactions for different native geometries. Our main finding is that, for G \bar{o} -type lattice polymers with $N = 48$ amino acids, the LR interactions play a crucial role in determining the folding rates and, most importantly, this effect is strongly dependent on native state's geometry. Indeed, we have found that, depending on the native geometry, the dispersion of the simulated folding times spans up to over ≈ 3 orders of magnitude when the relative strength of LR interactions varies from zero (only local interactions contribute to the native state's energy) to one (only LR interactions contribute to the native state's energy). We have also found that, depending on the native state's geometry, the set-up of LR contacts may be strongly associated with the previous formation of local contacts. The existence of this geometric coupling between local and LR contacts explains why the observed folding kinetics may depend rather weakly on the relative energetic contributions of local and long-range interactions. In proteins where this geometric coupling is stronger, the local contacts promote the establishment of LR contacts even when the LR interactions are not energetically favored.

The present article is organized as follows: The next section describes the model and methods. Afterwards we present and discuss the results of the simulations, and finally we draw the conclusions.

MODELS AND METHODS

Protein chains with $N = 48$ amino acids are modeled as self-avoiding walks on a three-dimensional infinite lattice. Amino acids are represented by beads of uniform size and the peptide bond, that covalently connects amino acids along the polypeptide chain, is represented by sticks of size equal to the lattice spacing. To mimic protein movement we use the so-called "kink-jump" move set including corner-flips, end and null moves, as well as crankshafts.²⁴ The G \bar{o} potential is used to model amino acid interactions, which means that, for a given target native structure, equal stabilizing energies (< 0) are ascribed to all the native contacts, that is, contacts between pairs of beads

which are present in the target, and neutral energies ($= 0$) are ascribed to all nonnative contacts, that is, contacts that are not present in the target structure. The total energy of a conformation $\Gamma = \{\vec{r}_i\}$ is then given by the contact Hamiltonian

$$H(\{\vec{r}_i\}) = \sum_{i>j}^N B_{ij} \Delta(\vec{r}_i - \vec{r}_j), \quad (1)$$

where the contact function, $\Delta(\vec{r}_i - \vec{r}_j)$, is unity if beads i and j form a native contact but are not covalently linked and is zero otherwise, and the interaction energy parameter is $B_{ij} = -\epsilon$.

The folding simulations follow the standard Monte Carlo (MC) Metropolis Algorithm.²⁵ Each MC run starts from a randomly generated unfolded conformation (typically with less than 10 native contacts) and the folding dynamics is traced by following the evolution of the fraction of native contacts, $Q = q/Q_{\max}$, where $Q_{\max} = 57$ (for chains with length $N = 48$) and q is the number of native contacts at each MC step. The folding time, t , is given by the first passage time (FPT), that is, the number of MC steps corresponding to $Q = 1.0$.

Native Structures

We consider three native structures, displaying different geometries as measured by the contact order parameter. These structures were found by homopolymer relaxation. In these MC simulations an homopolymeric chain (i.e., a polymer chain composed by beads of the same chemical type) is launched, at temperature $T = 0.7$, from a randomly generated conformation and relaxes, after some MC steps, to the minimum energy conformation. At each MC step a local random displacement of one or two beads, provided by the kink-jump move set, is accepted or rejected in accordance with the Metropolis rule. For each conformation the total energy is given by the contact Hamiltonian of Equation (1) where $\Delta = 1$ if beads are in contact but not covalently linked and is zero otherwise. The pairwise interaction energy parameter is $B_{ij} = -1.0$. For homopolymers of chain length $N = 48$ on a three-dimensional cubic lattice the most stable conformation, evolving under the Hamiltonian of Equation (1), is a cuboid with 57 contacts. Because this structure displays a maximum number of contacts it is generally referred to as a maximally compact structure.

To emphasize their different geometries, the low-CO (0.12) structure, Γ_1 , the intermediate-CO (0.19) structure, Γ_2 , and the high-CO structure (0.26) Γ_3 , are represented in Figure 1(a)–(c) through their contact maps²⁶ [in Fig. 1(d)–(f) the corresponding three-dimensional structures are provided as well]. The contact map, C , is an $N \times N$ matrix with entries $C_{ij} = 1$ if beads i and j are in contact and zero otherwise. In ref. 17 Gromiha and Sevaraj have found that for real two-state proteins the amino acids that are close in space and separated by at least 10 to 15 amino acids in sequence are important determinants of folding rates. Motivated by this finding we define a native contact between two beads i and j as a local contact if the backbone

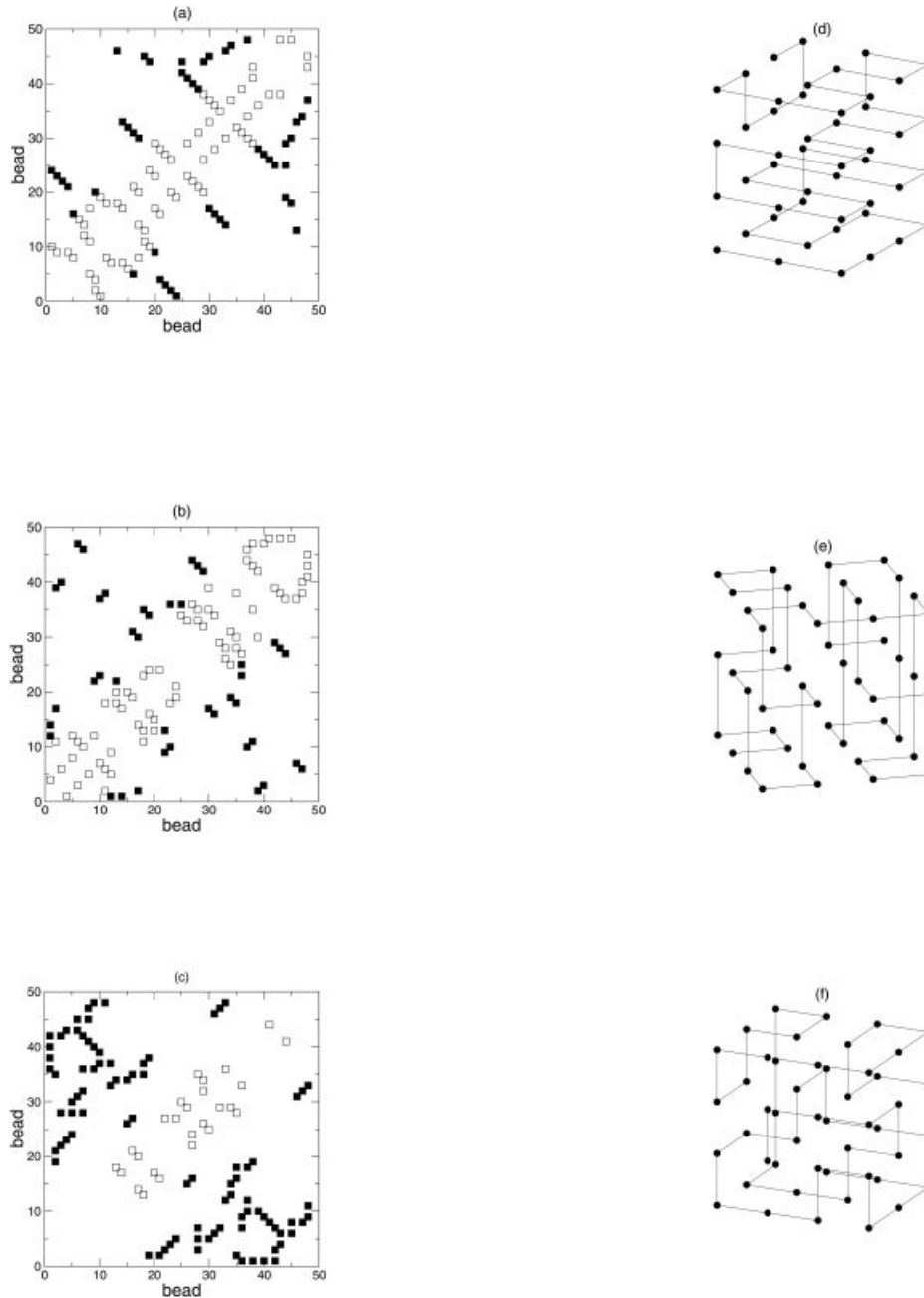


Fig. 1. Contact maps and three-dimensional representation of structures Γ_1 (a, d), Γ_2 (b, e), and Γ_3 (c, f). In the contact maps the black squares represent the long-range contacts and the white squares stand for the local contacts.

separation $|i - j|$ is such that $|i - j| \leq 10$ or as long-range (LR) contact if $|i - j| > 10$.

In Figure 1 the black squares represent the LR contacts while the white squares stand for the local contacts. The LRO parameter is 0.48 for Γ_1 , 0.44 for Γ_2 and 0.92 for Γ_3 . We stress that the number of LR and local contacts is approximately the same in targets Γ_1 and Γ_2 . The average LR contact length is 17.1 for Γ_1 , 20.1 for Γ_2 , and 26.5 for Γ_3 . Table I summarizes the geometric traits of the three target structures.

TABLE I. Contact Order, Fraction of Long-Range Native Contacts, Q_{LR} , Long-Range Order, and Average Long-Range Contact Length for Structures Γ_1 , Γ_2 , and Γ_3

Target	CO	Q_{LR}	LRO	$\langle i - j _{LR} \rangle$
Γ_1	0.129	0.40	0.48	17.1
Γ_2	0.190	0.35	0.42	20.1
Γ_3	0.259	0.77	0.92	26.5

Q_{LR} is the number of LR native contacts normalized to the total number of native contacts.

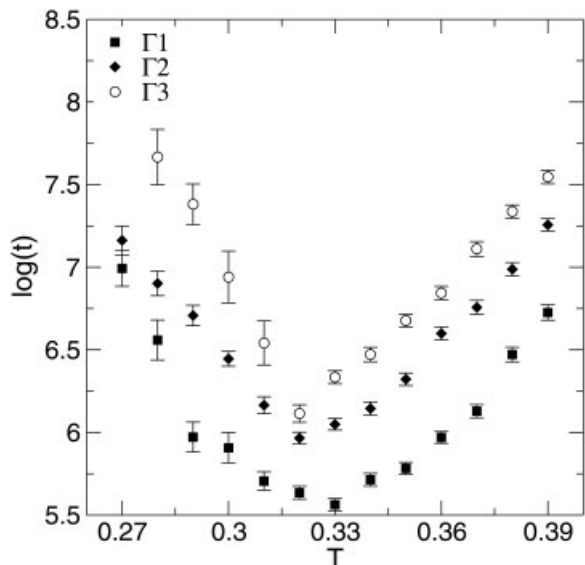


Fig. 2. Dependence of the logarithmic folding time, $\log_{10}(t)$, on the simulation temperature, T , for structures Γ_1 , Γ_2 , and Γ_3 .

NUMERICAL RESULTS

Simulation Temperature

The folding kinetics depends on the temperature parameter. Indeed, when the temperature is very high, all conformations are equally foldable and the kinetics becomes increasingly slower due to rapid interconversions (fluctuations) between unfolded states (in the high-temperature regime the folding time approaches the Levinthal time, that is, it becomes exponential in the number of accessible conformations). On the other hand, in the low-temperature regime, an Arrhenius-like behaviour, characterized by trapping into metastable states is expected (discussed in ref. 18). Therefore, for kinetically foldable proteins, there must exist an intermediate temperature that allows for a rapid folding. The existence of this temperature, called the optimal folding temperature, was reported in several studies for lattice models (sequence-specific and G \bar{O} models as well).^{18–21}

In the present study folding kinetics is studied at the optimal folding temperature T^* , that is, the temperature that minimizes the folding time, t . To determine T^* we performed MC simulations over a broad temperature range and ran a set of 100 MC simulations at each temperature, T . The folding time was then taken as the mean FPT to the native structure averaged over the 100 MC runs.

Figure 2 reports the dependence of the folding time on the folding temperature for each structure and $\epsilon = 0.5$. At the optimal folding temperature, the kinetics is not dominated by kinetic traps, and folding to the native state proceeds relatively fast.

We stress that, at $T = T^*$, the observed dispersion of folding times is rather small ($5.56 \pm 0.04 \leq \log_{10}(t) \leq 6.11 \pm 0.05$) and note that such behavior is typical of the G \bar{O} and other lattice (as well as off-lattice) models (ref. 8 and references therein).

The functional dependence of the folding time on the temperature is qualitatively similar for the three structures in the high- T regime. Note that in this regime one also observes a small dispersion of the folding times. However, the reported results show that in the low- T regime the dependence of the folding time on temperature is sensitive to the native state’s geometry. In particular, we have not observed folding to Γ_3 at low temperatures, $T < 0.28$.

The optimal folding temperature, on the other hand, appears to be a geometry independent parameter.

Folding Kinetics for Different Range Bias

In this section we investigate the role of LR and local contacts in the kinetics of protein folding by varying the relative contributions of LR and local interactions to the total energy in the following way: the energy of a conformation is given by

$$H(\{\tilde{r}_{ij}\}) = \sigma H_{\text{LR}}(\{\tilde{r}_{ij}\}) + (1 - \sigma)H_{\text{L}}(\{\tilde{r}_{ij}\}), \quad (2)$$

where the terms H_{LR} and H_{L} determine the overall energy contribution of long-range and local contacts to the conformation’s energy and are given by

$$H_{\text{LR(L)}}(\{\tilde{r}_{ij}\}) = - \sum_{i>j}^N \Delta_{\text{LR(L)}}(\tilde{r}_i - \tilde{r}_j), \quad (3)$$

where $\Delta_{\text{LR(L)}}(\tilde{r}_i - \tilde{r}_j)$ is unity if beads i and j form a LR (local) native contact and is zero otherwise. The parameter σ , that we shall call range bias parameter, takes values in $0.0 \leq \sigma \leq 1.0$. When σ is zero all LR interactions are “switched-off” and only local interactions contribute to the conformation’s total energy. The reverse situation is observed when $\sigma = 1.0$ as in this case only LR interactions contribute to the total energy. Conformation’s energies given by Equation (2) imply that the native’s state energy varies as a function of σ . Results plotted in Figure 3 illustrate the dependence of the native’s state energy on the range bias parameter for targets Γ_1 , Γ_2 , and Γ_3 . Although targets Γ_1 and Γ_2 have predominantly local contacts and thus their energy increases with σ , for target Γ_3 the lowest native state energy is observed when $\sigma = 1.0$. Because the native state’s energy depends on the range bias parameter we have determined, for each σ , the corresponding optimal folding temperature, T^* .

The dependence of the folding time on the range bias parameter is reported in Figure 4(a) for the three native geometries. For $\sigma < 0.20$ (resp. $\sigma < 0.10$) we have not observed folding to target Γ_3 (resp. Γ_2).

The behavior exhibited by target Γ_3 is easily explained: because approximately 80% of Γ_3 ’s native contacts are LR there is little competition (and therefore little frustration) between LR and local interactions. We stress that, in the present model, the competition between local and LR contacts results from the relative weight of the two types of interactions (which are always stabilizing, i.e., <0). The resulting frustration is therefore different from that of sequence-specific models where the energy of the local and

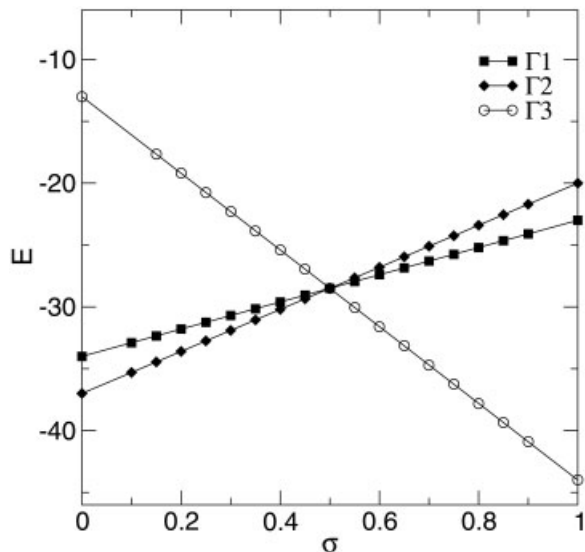


Fig. 3. Dependence of the native state's energy, E , on the range bias parameter σ for structures Γ_1 , Γ_2 , and Γ_3 .

of the LR pair interactions can be either stabilizing (i.e., <0) or not (i.e., $=0$ or >0).

The slight decrease in the folding time observed for $\sigma > 0.5$ is driven by the native state's energy (which, by decreasing with σ , results in a driving force to folding).

However, the effect of decreasing σ away from $\sigma = 0.5$ is equivalent to that of progressively "switching-off" the LR interactions and, in the limit of $\sigma = 0$, it actually corresponds forcing the structure to fold with only just 20% of its native interactions. In this case the driving force to folding becomes progressively small, which results in longer folding times and eventually, for $\sigma < 0.20$, folding failure. The observed threshold is smaller for target Γ_2 because, by contrast to the behaviour of target Γ_3 , the native state's energy decreases with σ (for $\sigma < 0.5$), and this effect balances that of switching-off the LR interactions.

The results obtained for the low- and intermediate-CO target structures, Γ_1 and Γ_2 , are more interesting. The corresponding curves are qualitatively similar but a closer inspection reveals an important difference, namely: for $\sigma < 0.5$ the dependence of the folding time on σ is much stronger for the intermediate-CO structure, Γ_2 . Indeed, in this case, one observes a remarkable three orders of magnitude dispersion of folding times, ranging from $\log_{10}(t_{\min}) = 5.76 \pm 0.05$ (for $\sigma = 0.65$) to $\log_{10}(t_{\max}) = 8.75 \pm 0.05$ (for $\sigma = 0.10$), by contrast with Γ_1 for which $\log_{10}(t_{\min}) = 5.50 \pm 0.08$ (for $\sigma = 0.70$) and $\log_{10}(t_{\max}) = 7.69 \pm 0.09$ (for $\sigma = 0.00$). We note that for both structures the folding time increases considerably more rapidly when σ decreases than when σ increases away from the minimum. However, in the latter case, the folding times do not deviate from each other by contrast with their behavior for $\sigma < 0.5$. We stress that for both geometries successful folding is still observed when $\sigma = 1.0$; this corresponds to "switching-off" all local interactions, which are more than half of the total number of interactions in both structures.

Folding Kinetics for Different Range Bias at Fixed Native Energy

To rule out differences in the folding dynamics driven by the stability of the native state we now investigate the contribution of LR and local interactions to the folding kinetics of structures Γ_1 , Γ_2 , and Γ_3 in the following way: the total energy of the native structure is kept fixed (and equal to $E = -28.5$, which is equivalent to taking $\epsilon = 0.5$ in Equation (1) while the relative contributions of LR and local interactions are varied over the whole range. We impose the fixed energy constraint by taking the total energy given by Equation (2) and using for the long-range and local Hamiltonians

$$H_{\text{LR(L)}}(\{\tilde{r}_i\}) = - \sum_{i>j}^N \epsilon(\sigma) \Delta_{\text{LR(L)}}(\tilde{r}_i - \tilde{r}_j), \quad (4)$$

with

$$\epsilon(\sigma) = \frac{0.5}{(1 - \sigma)Q_L + \sigma(1 - Q_L)} \quad (5)$$

where Q_L is the number of local native contacts normalized to the total number of native contacts. Again, the parameter σ determines the contribution of local and LR contacts to the total energy. For $\sigma = 0.0$ ($\sigma = 1.0$) only local (LR) contacts contribute to the total energy. However, $\epsilon(\sigma)$ that measures the interaction energy of all native contacts in $H_{\text{LR(L)}}$ varies with σ to keep the total energy of the conformation constant. Using Equations (2), (4), and (5) the energy per native contact is given by $\epsilon_L = (1 - \sigma)\epsilon(\sigma)$ if the contact is local while it is given by $\epsilon_{\text{LR}} = \sigma\epsilon(\sigma)$ for LR contacts. Figure 5 shows the dependence of ϵ_{LR} and ϵ_L on the range bias parameter for structures Γ_1 , Γ_2 , and Γ_3 .

We have studied the equilibrium population of states to investigate the native state's occupation probability at the optimal folding temperature as well as its dependence on σ . To this end long simulations (lasting up to 10^8 MC steps) were performed to ensure that data was collected under equilibrium conditions.¹² The results from these simulations (for the three considered targets) are reported in the histograms of Figure 6 for values of $\sigma = 0.3, 0.5, 0.7$. The height of each bar in the histograms, measures the probability occupancy, that is, the number of molecules (normalized to the total number of molecules collected in one run) with a fraction of native contacts Q . In all the considered cases most molecules are in the native state ($Q = 1.0$). However, when $\sigma = 0.3$, the native state of target Γ_1 , has a rather low probability occupancy (less than 0.5). Because the stability of the native state is estimated as being proportional to the probability of the chain being in the native conformation,¹² one can conclude that, for $\sigma = 0.3$, the native state of target Γ_1 is not very stable. We note that target Γ_3 , which has the largest fraction of long-range contacts, shows the highest native state occupation probability at all the three values of σ . This observation is in accordance with the idea that long-range contacts have a dominant role in stabilizing the native fold.

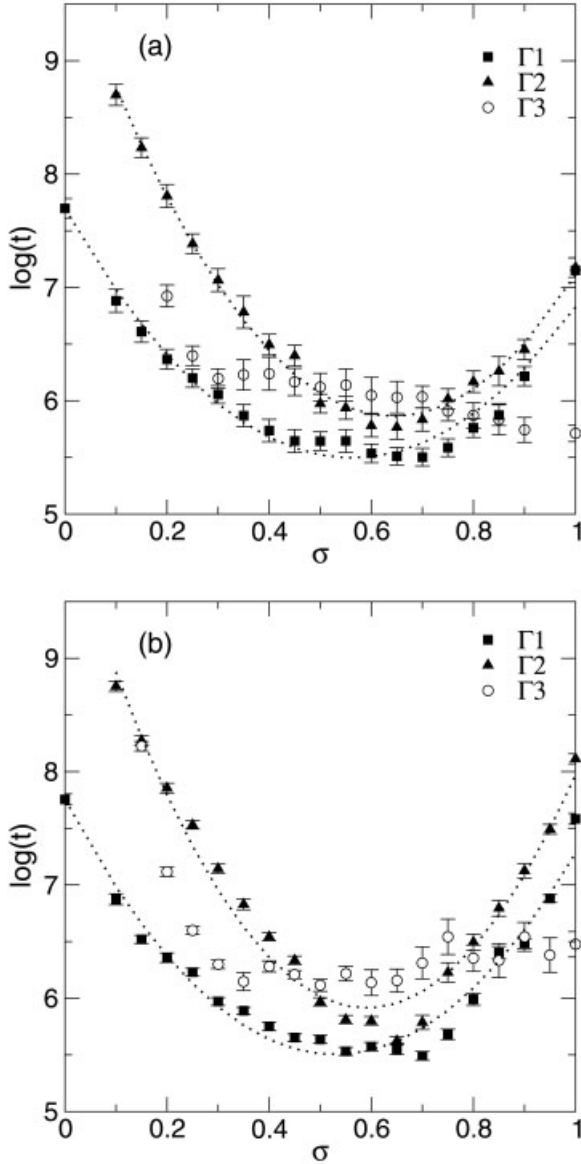


Fig. 4. (a) Dependence of the logarithmic folding time, $\log_{10}(t)$, on the range bias parameter σ for structures Γ_1 , Γ_2 , and Γ_3 with different native state's energies and with a fixed native state's energy (b).

Figure 4(b) shows the dependence of the folding time, t , on the range bias parameter for the three targets at fixed native state's energy. The conclusions drawn for the case of varying native state's energy hold equally well in the fixed energy case. In particular, the reported results confirm the trend for the dependence of Γ_3 's folding time on the range bias parameter. We should stress, however, that in the present case folding failure to the target is observed for $\sigma < 0.15$ in comparison with the varying energy model where no successful folding was observed if $\sigma < 0.20$. We ascribe this behavior to a more stabilizing (or equivalently, to a lower) native state's energy, which compensates the effect of "switching-off" the LR interactions. Hereafter we will restrict the discussion to the results for structures Γ_1 and Γ_2 . We note that the main difference between the fixed and

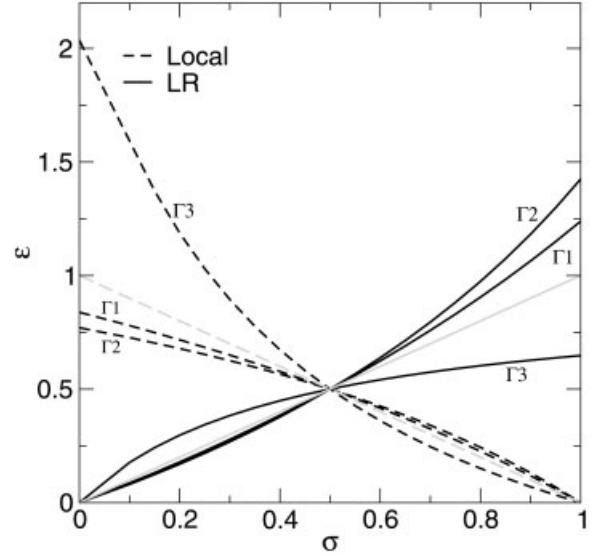


Fig. 5. Dependence of the ϵ_{LR} (energy per long range contact) and ϵ_L (energy per local contact) on the range bias parameter σ for structures Γ_1 , Γ_2 , and Γ_3 in the fixed energy model. Also shown (in light gray) the dependence of ϵ_{LR} and ϵ_L on σ in the case of the varying native energy model.

varying energies cases is that for $\sigma > 0.5$ the folding times are systematically longer (up to one order of magnitude for Γ_2) when the native state's energy is kept fixed. Recall from Figure 3 that when the native state's energy is allowed to vary it increases with σ up to $E = -23$ and $E = -20$ for targets Γ_1 and Γ_2 , respectively. The fixed native state's energy $E = -28.5$ is lower than the varying native energies in the range $\sigma > 0.5$. Should native energy play a significant role, the folding time's dependence on σ for $\sigma > 0.5$ would be less pronounced for the fixed native energy simulations, in sharp contrast with our findings. Instead, these are consistent with the idea that the kinetics of folding is dominated by the formation of LR contacts. As shown in Figure 5, in Γ_1 and Γ_2 the energy bias favoring LR contacts for $\sigma > 0.5$ is greater in the fixed energy case. This explains the differences in the behavior of the curves corresponding to these two targets in Figures 4(a) and 4(b).

From the overall results reported in Figure 4, we conclude that, by comparison with the local contacts, LR contacts play a crucial role, in driving the folding kinetics of small G \bar{o} -type lattice polymers. Moreover, the effect of LR contacts on the kinetics is strongly dependent on the native state's geometry.

Native Structure and the Geometric Coupling between Long-Range and Local Contacts

In this section we investigate the differences between the folding processes of targets Γ_1 and Γ_1 when σ is varied from zero to 1 to interpret the behaviour observed in the previous section.

Recall from Section II that our "reaction" coordinate is the fraction of native contacts Q . In general, Q works as a thermodynamic reaction coordinate by measuring closeness to the native structure in energetic terms only. As

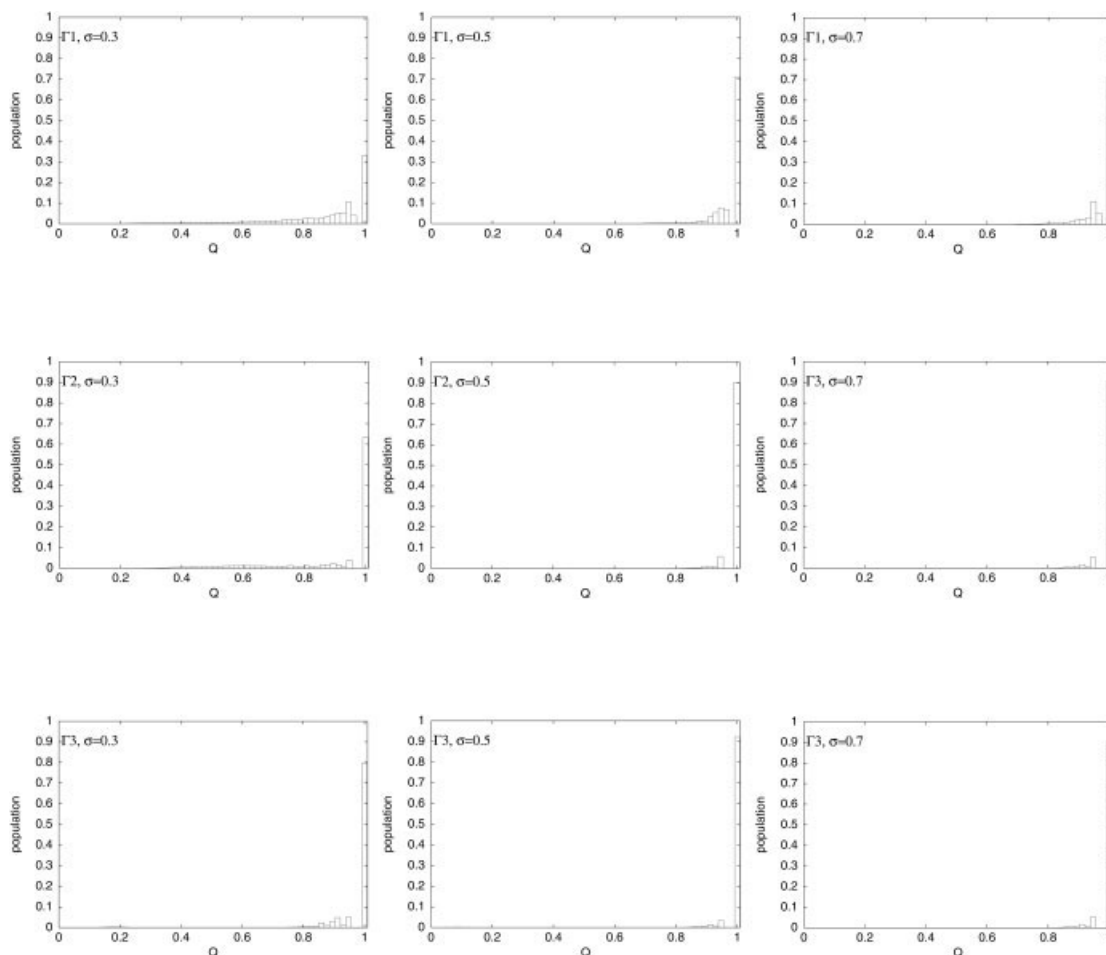


Fig. 6. Population histograms, for structures Γ_1 (first row), Γ_2 (second row), and Γ_3 (third row) and $\sigma = 0.3, 0.5$, and 0.7 at the optimal folding temperature. The native state, corresponding to $Q = 1.0$, is the dominant state for all structures at all values of σ . Except for structure Γ_1 at $\sigma = 0.3$ the native state's occupation probability is larger than 0.5 . Target Γ_3 , with the largest fraction of long-range contacts, exhibits the largest native state occupation probability at all values of σ . This observation is in line with the idea that long-range contacts have a dominant role in stabilizing the native fold.

argued in ref. 29, thermodynamic closeness does not necessarily imply kinetic proximity to the native structure unless the energy landscape is considerably smooth²⁸ (as it happens to be the case in the present study). Indeed, under such conditions one can take Q as a kinetic reaction coordinate so that it actually defines how quickly a conformation can convert into the native structure.²⁹ Thus, in what follows, we can assume that Q measures the kinetic progress towards the native state.

In Figure 7 we have plotted for targets Γ_1 and Γ_2 , and for three values of σ (namely, $0.5, 0.1$, and 1.0), the dependence on Q of the following kinetic quantities: the fraction of LR contacts, q_{LR} , the fraction of local contacts, q_L , and the normalized logarithmic folding time, $\log_{10} t^*$ (note that in this case the fractions of LR and local contacts are normalized to the total number of LR and local native contacts, respectively, and not to the total number of native contacts; therefore $q = 1.0$ when $Q = 1.0$ but in general, $q \neq Q$, and this is why the adopted notation is different from that used in the previous sections).

We start by observing the unbiased case, that is, $\sigma = 0.5$. The kinetics of local contact formation is similar in both targets with the fraction of local contacts starting from a much larger value than that of LR ones. However, long-range contacts form considerably earlier in Γ_1 and, in this case, the kinetics of LR contacts follows that of q_L . In both cases, the normalized folding time is controlled by the formation of local contacts. For $\sigma = 1.0$ local interactions are switched-off, and this results in an effective slowing down of the corresponding kinetics in both targets. Note that, in Γ_1 , q_{LR} grows extremely quickly reaching $\approx 90\%$ relatively early in the folding process (when $Q = 0.58$) when compared with the behaviour exhibited for $\sigma = 0.5$ (90% when $Q = 0.92$). However, this early boost in q_{LR} does not promote a stable structure formation as it subsequently drops down to $q_{LR} = 0.84$ (for $Q = 0.86$) and is then forced to follow the kinetics of local contact formation. For this value of σ , the folding time is controlled by the setting up of LR contacts in Γ_2 and by that of local contacts in Γ_1 . Finally, when $\sigma = 0.1$, both targets exhibit a similar

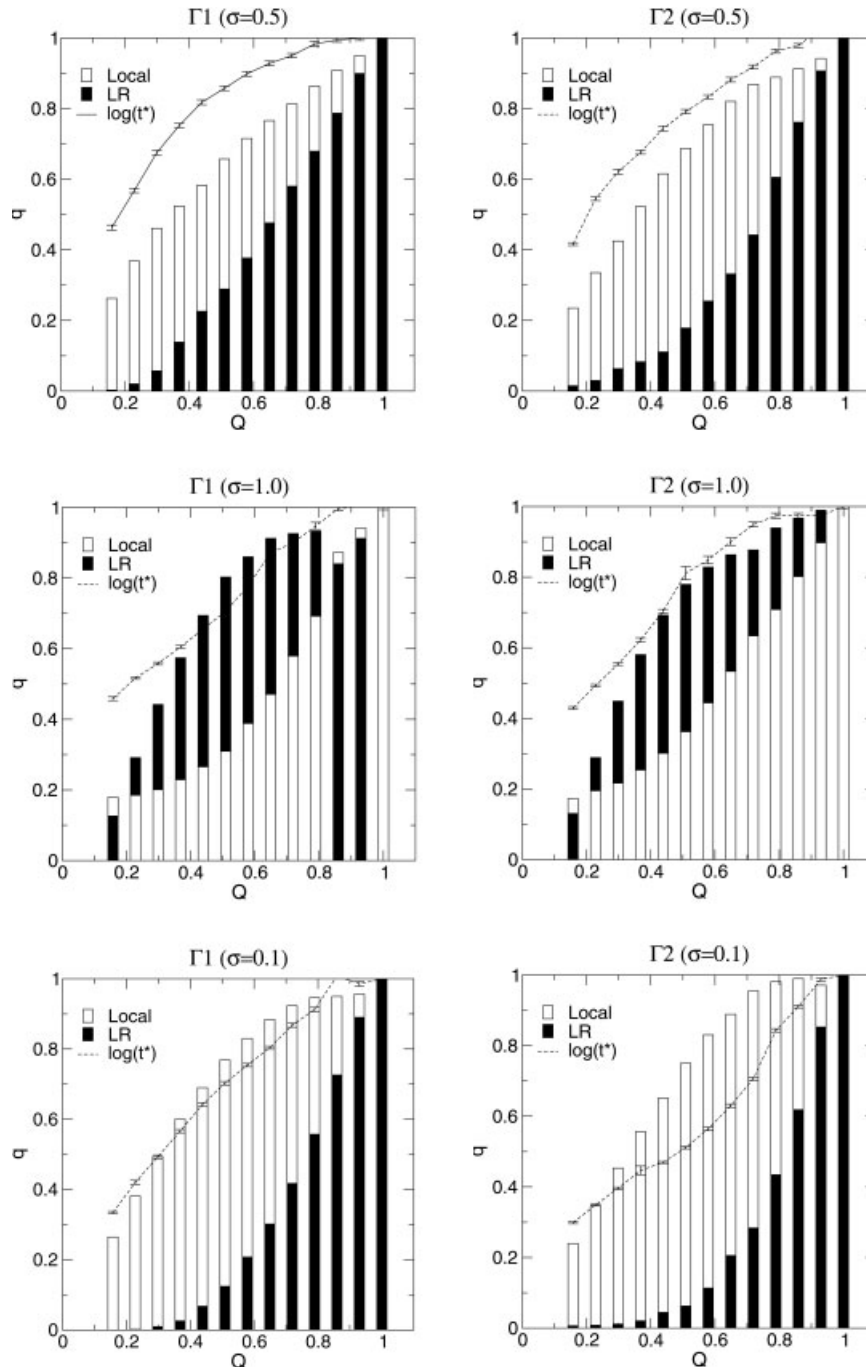


Fig. 7. Dependence of the fractions of long-range (LR) and local contacts on the fraction of native contacts, Q , for targets Γ_1 , Γ_2 , and $\sigma = 0.5, 1.0$, and 0.1 . Note that q is q_{LR} (i.e., the fraction of LR contacts) for the black bars and q_L (i.e., the fraction of local contacts) for the white bars. q_{LR} (q_L) is the number of LR (local) contacts normalized to the total number of LR (local) contacts in each native structure. Also shown is the dependence of $\log_{10}(t^*)$ on Q where t^* is folding time at each Q normalized to the folding time at $Q = 1.0$.

dependence of q_L on Q but the kinetics of q_{LR} is slowed down considerably in Γ_2 . Again, the folding time is controlled by q_L in Γ_1 and by q_{LR} in Γ_2 , but for Γ_2 , the setting-up of LR contacts is much slower than in previous cases.

We interpret these observations in the following way: in target Γ_1 there is a strong geometric coupling between the formation of local and LR contacts, which means that the

establishment of LR contacts is promoted by the establishment of local contacts. On the other hand, in target Γ_2 , there is no such coupling and this results in an overall kinetics, which is more sensitive to changes in the energy interaction parameters. In particular, in Γ_2 , local contacts are not capable of promoting the setting-up of LR contacts when the LR interactions are highly penalized energetically.

cally (recall that we did not observe successful folding to Γ_2 when $\sigma < 0.10$).

CONCLUSIONS AND FINAL REMARKS

In this article we have revisited the Gō model to investigate, by means of a new approach, the role of long-range (LR) and local interactions in the folding kinetics. We have focused our analysis on lattice-polymers with chain length $N = 48$ because, as in real two-state folders, these models exhibit relatively smooth energy landscapes. We studied the changes in the folding process induced by unbalancing the contributions of local and LR interactions to the native state's energy. Our results strongly suggest that LR interactions play a dominant role in the folding kinetics. Indeed, we observe a decrease in the folding rates, or equivalently, an increase in the folding time, which is clearly more pronounced when the contribution of the LR interactions (relative to that of the local interactions) to the native state's energy is progressively decreased towards zero. We have found that this effect is essentially independent on the native state's energy. However, the kinetic response to decreasing the relative contributions of LR interactions is strongly dependent on the target geometry. We have selected our target geometries on the basis of differing contact order parameters. In the high-CO target, Γ_3 , LR contacts are the vast majority (44 out of 57 native contacts), and this results in a trivial kinetic response: when LR interactions are strengthened relative to the local ones there are no significant changes in the folding rates; on the other hand, a strong increase in the folding rates (eventually resulting in folding failure) arises when they are weakened. Interesting behavior occurs in the folding kinetics of the other two structures, the low- and intermediate-CO targets, Γ_1 and Γ_2 , respectively. In both structures local contacts dominate and both exhibit a similar fraction of local and LR contacts. However, in the intermediate-CO target the kinetics is much more sensitive to weakening the LR interactions; indeed, in this case we have observed a remarkable three orders of magnitude dispersion in the folding times, although still two orders of magnitude smaller than the dispersion of folding times of real two-state folders (≈ 5 orders of magnitude).¹⁰

The topomer search model (TSM) for protein folding (reviewed in ref. 31) considers that the folding time is determined by the diffusive search for the ensemble of unfolded structures that share a similar, global topology with the native state (the native topomers).³² Achieving the native topomer corresponds to surmounting the rate-limiting step in folding, which is followed by the zippering of specific local native contacts, a process that rapidly leads to the native structure. Therefore, according to the TSM, the rate at which an unfolded protein diffuses between distinct topologies is much slower than the rate at which local structural elements form. Recent results obtained through numerical simulations on the diffusion of Gaussian chains by Makarov et al.^{31,33} suggest, in the context of this model, that the logarithmic folding rate grows linearly with the number N_{LR} of

LR contact pairs in the native structure, which define the topomer. Makarov et al.³¹ have investigated if the TSM correlates well with the folding rates of the 24 two-state folders previously studied by Plaxco et al.¹⁰ To determine N_{LR} for each protein the authors have considered as LR a native contact where the amino acids are separated by at least 12 or more residues along the protein backbone. A considerably strong correlation $r = 0.88$ was found between the logarithmic folding rates and N_{LR} ,³¹ suggesting that the TSM is indeed a good model for reproducing two-state folding rates. Our results are in broad agreement with the TSM in the sense that, irrespectively of target geometry, we have found that decreasing, versus increasing, the relative weight of LR interactions produces a more pronounced increase of the folding times. However, we have also found evidence of a folding mechanism (operating on the lattice) that is different from the one proposed by the TSM. According to the TSM, the step that determines the folding rates is the formation of the LR contacts in the native topomer. After this step a rapid zippering of the local contacts occurs and the native structure forms. Our results show that, depending on native geometry, the formation of LR contacts may be more strongly coupled with the formation of the local contacts. This is well illustrated with the behavior of target Γ_1 when $\sigma = 0.1$ (Fig. 7). For this value of σ the LR contacts are strongly energetically penalized, and the folding time is controlled by local contact formation. This is not observed for target Γ_2 , where under the same conditions ($\sigma = 0.1$) the folding time is controlled by LR contact formation (Fig. 7), in agreement with the TSM. Another evidence in support of the coupling between local and LR contact formation in target Γ_1 is the fact that, again for $\sigma = 0.1$, LR contact formation is much more rapid for target Γ_1 than for target Γ_2 . We note that this particular aspect of the folding process in lattice models has not been explored in previous simulation efforts.

In a recent study Micheletti et al.³⁴ have introduced a novel method, the so-called “geometrical variational principle,” to investigate the role of native geometry in guiding the protein to the native fold. This study consisted in computing the number of structures that share a certain structural similarity with a given native structure (the structural similarity between a structure and the fixed native fold is measured by the fraction of native contacts Q in that structure). The authors have called this measure the density of overlapping conformations (DOC). The most important result from this study was the finding that the DOC of real natural folds is always much larger (at any value of Q) than the one found for artificially generated structures (with equal chain length and equal number of contacts but differing in the fractions of local and nonlocal contacts). Moreover, the authors have also found that, for $Q \approx 0.5$, the DOC of real folds is very close to its maximum value and that this “extremality” of the DCO is related with a high content in secondary structure-like motifs (α -helices and β -sheets). In a subsequent study Maritan et al.³⁵ have

applied a “dynamical variational principle” (DVP) to search for rapid folders in conformational space. The authors have found, in the context of a G \bar{O} model on an fcc lattice, that decreasing folding times are associated with increasing secondary structure content (in agreement with Micheletti’s results) and with decreasing contact order. This finding shows that the application of the DVP to search for kinetically foldable proteins results in the emergence of structures with predominantly helical order (i.e., with a high content in local contacts). Because our results were obtained for a cubic lattice a direct comparison with Maritan’s finding is not possible. However, in the contact map of Figure 1(a), corresponding to Γ_1 , one can clearly identify a pattern that resembles the signature of α -helices namely, the existence of thick bands parallel to the diagonal. The fact that structure Γ_1 shows the quickest folding time for all values of the LR interaction strength is therefore in broad agreement with Maritan’s results.

The existence of a geometric coupling between local and LR contacts might have implications in what concerns the understanding of protein evolution in the sense that it provides a possible mechanism for the emergence of the mutational robustness in proteins. A biological system is said to be robust to mutations if it continues to function after genetic changes in its parts. Native structures endowed with a mechanism of local-LR contact coupling are naturally more capable of exhibiting a fast adaptation to mechanisms of biomolecular variation (point mutations, insertions, deletions, etc.) that change the amino acid sequence (i.e., that change the set of amino acid interactions) in the following sense. If the geometric coupling between local and LR contacts exists, one expects the protein’s foldability (the protein’s ability to fold at a reasonably fast rate, which is indeed an evolutionary advantage) to be less affected by changes in the way the amino acids interact, because when the LR contacts become energetically penalized, as a result of sequence changes, the formation of local contacts acts as a driving force for the establishment of the LR ones.

Finally, it would be interesting to investigate the interplay between target geometry and favored native contact interactions in more realistic models, where not only the dispersion of folding times of real proteins is reproduced as well as other aspects observed in the folding of real two-state folders such as the thermodynamic and the kinetic cooperativities.³⁰ A simple model that is a step in this direction is that of Kaya and Chan who used a modified G \bar{O} -type potential, involving nonadditive multi-body interactions, to study the folding dynamics of 27-mers on a cubic lattice.⁸ When applied to a pool of targets comprising 97 native geometries, chosen on the basis of their CO parameters, Kaya and Chan’s model yielded folding rates spanning more than 2.5 orders of magnitude. Furthermore, this model also exhibited thermodynamic cooperativity and linear chevron plots (i.e., kinetic cooperativity) similar to those observed in experiments with real proteins.

ACKNOWLEDGMENTS

P.F.N.F. is grateful to Prof Hue Sun Chan for helpful comments on a preliminary version of the present work.

REFERENCES

1. Plaxco KW, Simmons KT, Baker D. Contact order, transition state placement and the refolding rates of single domain proteins. *J Mol Biol* 1998;277:985–994.
2. Du R, Pande VS, Grosberg AY, Tanaka T, Shakhnovich E. On the role of conformational geometry in protein folding. *J Chem Phys* 1999;111:10375–13080.
3. Baker D. A surprising simplicity to protein folding. *Nature* 2000;405:39–42.
4. Dokholyan NV, Li L, Ding F, Shakhnovich EI, Topological determinants of protein folding. *Proc Natl Acad Sci USA* 2002;99:8637–8641.
5. Miller EJ, Fischer KE, Marqusee S. Experimental evaluation of topological parameters determining protein-folding rates. *Proc Natl Acad Sci USA* 2002;99:13059–10363.
6. Faisca PFN, Ball RC. Topological complexity, contact order and protein folding rates, *J Chem Phys* 2002;117:8587–8591.
7. Weikl TR, Dill KA. Folding rates and low entropy routes of two-state proteins. *J Mol Biol* 2003;329:585–598.
8. Kaya H, Chan HS. Contact order dependent protein folding rates: kinetics consequences of a cooperative interplay between favorable nonlocal interactions and local conformational preferences. *Proteins* 2003;52:524–533.
9. Faisca PFN, Telo da Gama MM, Ball RC. Folding and form: insights from lattice simulations. *Phys Rev E* 2004;69:051917.
10. Plaxco KW, Simmons KT, Ruczinski I, Baker D. Topology, stability, sequence and length: defining the determinants of two-state protein folding kinetics. *Biochemistry* 2000;39:11177–11183.
11. G \bar{O} N, Taketomi H. Respective roles of short- and long-range interactions in protein folding. *Proc Natl Acad Sci USA* 1978;75: 559–563.
12. Abkevich VI, Gutin AM, Shakhnovich EI. Impact of local and non-local interactions on thermodynamics and kinetics of protein folding. *J Mol Biol* 1995;252:460–471.
13. Doyle R, Simons K, Qian H, Baker D. Local interactions and the optimization of protein folding. *Proteins* 1997;29:282–291.
14. Gromiha MM and Selvaraj S. Importance of long-range interactions in protein folding. *Biophys Chem* 1997;77:49–68.
15. Unger E, Moulton J. Local interactions dominate folding in a simple protein model. *J Mol Biol* 1996;259:988–994.
16. Govindarajan S, Goldstein RA. Optimal local propensities for model proteins. *Proteins* 1995;22:413–418.
17. Gromiha MM, Selvaraj S. Comparison between long-range interactions and contact order in determining the folding rate of two-state folders: application of long-range order to folding rate prediction. *J Mol Biol* 2001;310:27–32.
18. Gutin AM, Abkevich VI, Shakhnovich EI. Chain length scaling of protein folding. *Phys Rev Lett* 1996;77:5433–5436.
19. Gutin A, Sali A, Abkevich V, Karplus M, Shakhnovich EI. Temperature dependence of the folding rate in a simple protein model: search for a “glass” transition. *J Chem Phys* 1998;108:6466–6483.
20. Cieplak M, Hoang TX, Li MS. Scaling of folding properties in simple models of proteins. *Phys Rev Lett* 1999;83:1684–1687.
21. Faisca PFN, Ball RC. Thermodynamic control and dynamical regimes in protein folding. *J Chem Phys* 2002;116:7231–7238.
22. Gillespie B, Plaxco KW. Nonglassy kinetics in the folding of a simple single-domain protein. *Proc Natl Acad Sci USA* 2000;97: 12014–12019.
23. Shea JE, Onuchic JN, Brooks CL. Probing the folding free energy landscape of the src-SH3 protein domain. *Proc Natl Acad Sci USA* 2002;99:16064–16068.
24. Landau DP, Binder K. *A Guide to Monte Carlo simulations in statistical physics*. Cambridge: Cambridge University Press; 2000.
25. Metropolis N, Rosenbluth AW, Rosenbluth MN, Teller AH, Teller E. Equation of state calculations by fast computing machines. *J Chem Phys* 1953;21:1087–1092.
26. Saitoh S, Nakai T, Nishikawa K. A geometric constraint approach for reproducing the native backbone conformation of a protein. *Proteins* 1993;15:191–204.

27. Fan K, Wang J, Wang W. Modeling two-state cooperativity in protein folding. *Phys Rev E* 2001;041907.
28. Jewett AI, Pande VS, Plaxco KW. Cooperativity, smooth energy landscapes and the origins of topology-dependent protein folding rates. *J Mol Biol* 2003;326:247–253.
29. Chan HS, Dill KA. Protein folding in the landscape perspective: Chevron plots and non-arrhenius kinetics. *Proteins* 1998;30:2–33.
30. Chan HS, Shimizu S, Kaya H. Cooperativity principles in protein folding. *Methods Enzymol* 2004;380:350–379.
31. Makarov DE, Plaxco KW. The topomer search model: a simple, quantitative theory of two-state protein folding kinetics. *Protein Sci* 2003;12:17–26.
32. Debe DA, Carlson MJ, Goddard WA. The topomer-sampling model of protein folding. *Proc Natl Acad Sci USA* 1999;96:2596–2601.
33. Makarov DE, Metiu H. A model for the kinetics of protein folding: kinetic Monte Carlo simulations and analytical results. *J Chem Phys* 2002;116:5205–5216.
34. Maritan A, Micheletti C, Banavar, JR. Role of secondary motifs in fast folding polymers: a dynamical variational principle. *Phys Rev Lett* 2000;3009–3012.
35. Micheletti C, Banavar JR, Maritan A, Seno F. Protein structures and optimal folding from a geometrical principle. *Phys Rev Lett* 1999;3372–3375.